Foams Stabilized by Aquivion™ PFSA: Application to Interfacial Catalysis for Cascade Reactions

Andong Feng, Dmytro Dedovets, Shi Zhang, Jin Sha, Renate Schwiedernoch, Jie Gao, Yunjiao Gu, and Marc Pera-Titus*

Foams are attractive platforms for engineering gas–liquid–solid catalytic micro-reactors with enhanced triphasic contact. In this study, the foaming properties of surface-active Aquivion™ perfluorosulfonic acid resin (Aquivion™ PFSA) are unraveled. Stable aqueous and non-aqueous foams are prepared driven by hydrogen bond interactions between Aquivion™ PFSA and protic solvents (e.g., benzyl alcohol, aniline, water). In light of these unique properties, a catalytic foam system for one-pot cascade deacetalization–hydrogenation reactions is designed. As proof of concept, benzaldehyde dimethyl acetal is converted into benzyl alcohol with 84% overall yield at room temperature in a foam system in the presence of Aquivion™ PFSA and Pd/SiO$_2$ catalysts, whereas the yield is halved in a non-foam system. The enhanced reaction efficiency is attributed to a marked increase in interfacial area of the foam system and preferential location of catalytic acid centers at the gas–liquid interface.

1. Introduction

Gas–liquid–solid (G–L–S) catalytic reactions are widespread in the chemical industry for the synthesis of fine chemicals and depollution. Typical examples are the hydrodesulphurization of naphtha, the partial oxidation of liquid hydrocarbons with air or O$_2$, and the wet air oxidation of pollutants for water remediation.[1] Conventional gas–liquid–solid catalytic reactors comprise packed beds (e.g., trickle beds, bubble columns), stirred tank and bubble column slurry reactors, and fluidized beds.[2]

These technologies often suffer from low gas solubility in liquids, and mass/heat transfer resistances due to low gas–liquid and liquid–solid specific interface areas.[3] As a way out, continuous flow micro-reactors, catalytic membrane reactors and microbubble generators can promote the gas–liquid interfacial area and enhance catalytic reactions,[4] but require complex equipment. Therefore, it is highly desirable to develop a simple and cheap strategy to enhance the catalytic performance.

Liquid foams are multiphase systems consisting of disperse gas bubbles in a continuous liquid phase.[5] Aqueous foams can be readily stabilized by a variety of surface-active particles, including partially hydrophobic silicas, polymers and surfactant crystals.[6] In contrast, fewer reports are available on non-aqueous foams due to the low surface tension of organic liquids.[7] Since particles coated by hydrocarbon-containing groups can be wetted by many oils, the preparation of particle-stabilized oil foams is much more challenging than aqueous foams.[5b,8] To generate repellence against oil on the particle surface, fluorinated particles such as polytetrafluoroethylene, oligomeric tetrafluoroethylene and particles bearing fluoro-carbon chains, have been recently used, allowing the stabilization of non-aqueous foams.[9] Owing to the low surface energy of fluorinated chains, stable air-in-oil foams can be obtained in oils with intermediate surface tension. However, few studies have been reported on non-aqueous foams in ethanol with low surface tension, and polar solvents with intermediate surface tension (e.g., benzyl alcohol and ethylene glycol).[10]

Particle-stabilized foams can be used to engineer gas–liquid-solid catalytic microreactors with an enhanced triphasic contact at the nanoscale. Yuan and co-workers synthesized particles based on monodisperse Au nanoparticles embedded in polyoxometalate anion [PV$_2$Mo$_{10}$O$_{40}$]$^{5-}$ assembled with rigid tripodal ligand by electrostatic interactions.[11] The multifunctional catalyst could self-assemble at the O$_2$/water interface, stabilizing bubbles. This catalytic system showed high activity in the oxidation of aliphatic/aromatic alcohols into aldehydes and ketones. Likewise, Yang and co-workers synthesized silica particles modified with octyl and triamine groups stabilizing gas bubbles in water.[12] By incorporating Pd or Au nanoparticles, the particles were active for aqueous hydrogenation and oxidation reactions in H$_2$ and O$_2$ foams, respectively, under stirring at high particle concentration (7.5–12.5 wt%). The catalytic foams exhibited an enhanced activity compared to conventional multiphasic reactors, which was attributed to a pronounced

A. Feng, J. Sha, R. Schwiedernoch, J. Gao, Y. Gu, M. Pera-Titus
Eco-Efficient Products and Processes Laboratory (E2P2L)
UMI 3464 CNRS-Solvay
3966 Jin Du Road, Xin Zhuang Ind. Zone, Shanghai 201108, China
E-mail: marc.pera-titus-ext@solvay.com
D. Dedovets, S. Zhang
Laboratoire du Futur (LOF)
UMR 5258 CNRS-Solvay-Univ. Bordeaux
178 Av. Dr Albert Schweitzer, Pessac Cedex 33608, France
M. Pera-Titus
Cardiff Catalysis Institute
School of Chemistry
Cardiff University
Main Building, Park Place, Cardiff CF10 3AT, UK

The ORCID identification number(s) for the author(s) of this article can be found under https://doi.org/10.1002/admi.202200380.

increase of the reaction interface area. Very recently, some of us have developed fluorinated silica particles incorporating Pd nanoparticles able to generate foams in non-aqueous solvents. The particles exhibited 7–10 times activity increase in the aerobic oxidation of aromatic and aliphatic alcohols in O_2 at ambient pressure compared to non-foam systems.[13]

Aquivion[TM] perfluorosulfonic acid (PFSA) resin is a superacid ionomer with an acid strength comparable to that of sulfuric acid (Hammett acidity ≈ −12).[14] It is a semi-crystalline thermoplastic copolymer of tetrafluoroethylene and sulfonyl fluoride vinyl ether produced by Solvay Specialty Polymers. Aquivion[TM] PFSA solid acid catalyst, formulated as coarsely grained powder (e.g., PW98), has been studied for catalysis in a variety of acid-catalyzed reactions.[15] Moreover, Aquivion[TM] dispersion (e.g., D98) has affinity to both water and hydrophobic substrates.[16] Aquivion[TM] PFSA has demonstrated surface activity for stabilizing emulsions, affording biphasic reactions at the oil/water and oil/oil interface.[17] We hypothesize that this unique property may offer the possibility of generating foams both in water and organic solvents.

Herein, we first investigated the foaming behavior of an Aquivion[TM] PFSA dispersion in a variety of solvents. The key parameters (e.g., concentration, temperature, solvent) controlling foamability and foam stability were studied in detail. Next, relying on the unique surface-active and acid properties of Aquivion[TM] D98-20BS-P, we designed a foam system for one-pot cascade deacetalization–hydrogenation reactions by synergistically combining Aquivion[TM] PFSA with a heterogeneous palladium catalyst.

2. Results and Discussion

2.1. Characterization of Aquivion[TM] D98-20BS-P

To obtain a surface-active material allowing generation of stable foams in a variety of solvents, an Aquivion[TM] D98-20BS dispersion in water was lyophilized overnight, and the resulting resin was characterized in detail. Figure S1 (Supporting Information) shows an image of the resulting white powder (denoted as Aquivion[TM] D98-20BS-P). The weight-average molecular weight (M_w) of Aquivion[TM] D98-20BS-P is 152 kDa with a polydispersity index (PDI) of 1.8 as measured by GPC (Figure S2, Supporting Information).

The thermal profile of Aquivion[TM] D98-20BS-P measured by TG analysis matches well earlier measurements on Aquivion[TM] PW98 (coarsely grained powder) (Figure S3a, Supporting Information).[14a,17b–c] Two primary mass loss processes are observed: a first weight loss below 160 °C attributed to the evaporation of adsorbed water, and a second weight loss in the range 280–550 °C ascribed to the decomposition of the side chain and perfluorocarbon backbone.

The surface composition of Aquivion[TM] D98-20BS-P was inspected by FT-IR spectroscopy (Figure S3b, Supporting Information). The IR spectrum shows two intense bands at 1147 and 1203 cm^{-1} that are ascribed to the C–F stretching mode.[14a,18] The medium intensity band around 1050 cm^{-1} is attributed to the asymmetric stretching mode of S–O groups.[19] Besides, a characteristic band attributed to C–O–C species is visible at 968 cm^{-1}. Finally, the broad vibrational band in the region

of 3800–2800 cm^{-1} belongs to O–H stretching modes, which reflects the hydrophilic behavior of the sample ascribed to sulfonic acid groups.

XPS measurements were carried out to gain insight into the chemical composition of Aquivion[TM] D98-20BS-P. The bands in the wide scan of Aquivion[TM] D98-20BS-P confirm the presence of C, O, S, and F elements (Figure S4, Supporting Information). The C 1s spectrum can be deconvoluted into three different peaks with binding energies of 284.9, 288.4, and 291.6 eV, corresponding to skeletal C—C bonds, C—O bonds in side chains, and the perfluorocarbon backbone (CF_2-CF_2), respectively.[17b,20] The peak at ≈169.3 eV can be attributed to sulfonic acid groups.[20b,21] Meanwhile, the F 1s spectrum of Aquivion[TM] D98-20BS-P exhibits a single and symmetric peak at 688.6 eV, which is ascribed to fluorine atoms present in the polymer backbone.

The structural features of Aquivion[TM] D98-20BS-P were investigated by liquid ^{19}F and ^{1}H NMR (Figure S5, Supporting Information). The ^{19}F NMR spectrum is consistent with earlier observations on Aquivion[TM] PFSA.[17c,22] The resonance bands at −78.8 and −138.1 ppm are signatures of OCF_2 groups in side chains and CF groups in the backbone of Aquivion[TM] PFSA, respectively. A band centered at 123.1 ppm is clearly visible and is typically ascribed to CF_2-CF_2 units in fluoropolymers.[23] In addition, the signal at −118.3 ppm corresponds to SCF_2 and CCF_2 groups. The ^{1}H NMR spectrum of Aquivion[TM] D98-20BS-P displays a band centered at 5.6 ppm, which is indicative of the presence of SO_3H groups.

2.2. Foamability of Aquivion[TM] D98-20BS-P

2.2.1. Foaming Studies in Benzyl Alcohol

Previous studies demonstrated that polytetrafluoroethylene and fluorinated particles can stabilize foams in solvents of intermediate surface tension (30–45 mN m^{-1}) such as toluene, benzene and benzyl acetate.[8,9a–c] Nonetheless, very few studies succeeded the stabilization of foams in aromatic solvents with relatively high polarity (e.g., benzyl alcohol and aniline).[10b]

The foaming properties of Aquivion[TM] D98-20BS-P were studied by hand shaking and were compared to those attained using other stabilizers. In benzyl alcohol, Aquivion[TM] D98-20BS-P can generate decent foam volume with a lifetime up to 8 h (**Figure 1**). In contrast, Aquivion[TM] PW98, formulated as a coarse powder, can hardly disperse in benzyl alcohol, and thus is unable to generate foam. Likewise, polytetrafluoroethylene (PTFE), possessing no polar groups, can neither disperse in benzyl alcohol nor stabilize any foam. These results underline the significance of the polar group in Aquivion[TM] PFSA, favoring the interaction with benzyl alcohol and foam formation.

To better understand the effect of Aquivion[TM] D98-20BS-P on foamability and foam stabilization in benzyl alcohol, we tested a range of commonly used surfactants, including sodium dodecylbenzenesulfonate (SDBS), dodecyltrimethylammonium bromide (DTAB), polyoxyethylene (10) tridecyl ether (POTE), perfluorooctanoic acid (PFOA), and myristic acid (MA). Almost no foam is generated with cationic surfactant (DTAB), non-ionic surfactant (POTE), and fatty acid (MA). In contrast,
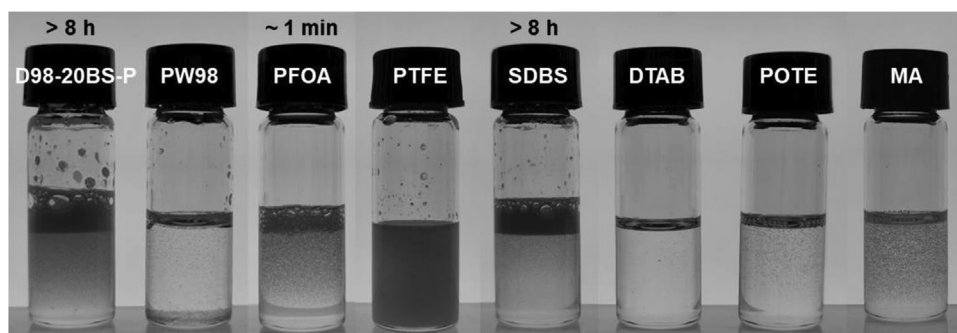
Figure 1. Foamability of different stabilizers in benzyl alcohol (1 wt%) after hand shaking. The foam volume was homogeneous within the flask in all the measurements.

anionic surfactants (SDBS and PFOA) exhibit good foamability in benzyl alcohol, even if foam stability differs: 8 h for SDBS versus only 1 min for PFOA. Among all the different agents, only Aquivion[TM] D98-20BS-P, SDBS and PFOA exhibit good foamability in benzyl alcohol, which is correlated to a decrease of surface tension of benzyl alcohol (**Table 1**, entries 2–4). The remaining agents (e.g., Aquivion[TM] PW98, PFTE) exert almost no effect on the surface tension (Table 1, entries 5–9), and no foams are generated in benzyl alcohol.

Based on these results, we can reasonably assume that hydrogen bond interactions between benzyl alcohol molecules and Aquivion[TM] D98-20BS-P favor foam generation. By neutralizing Aquivion[TM] D98-20BS-P with 10 µL of a strong base (e.g., ethylenediamine, NaOH, NH$_3$), a turbid suspension is obtained leading to particle precipitation. Precipitation is driven most likely by the formation of bridges between Aquivion[TM] D98-20BS-P and the base, resulting in complete lack of foamability in benzyl alcohol (**Figure 2**).

2.2.2. Effect of Aquivion[TM] D98-20BS-P Concentration

The effect of Aquivion[TM] D98-20BS-P concentration on the foaming properties was first investigated by hand shaking. The foamability increases progressively with the Aquivion[TM]

Table 1. Surface tension of benzyl alcohol after addition of different agents (1 wt%).

Entry	Agent	Surface tension [mN m^{-1}]
1	Pure benzyl alcohol	38.9
2	Aquivion[TM] D98-20BS-P	33.6
3	PFOA	31.4
4	SDBS	36.4
5	Aquivion[TM] PW98	38.3
6	PTFE	38.7
7	DTAB	38.7
8	POTE	38.6
9	MA	38.7

Nomenclature: DTAB, dodecyltrimethylammonium bromide; MA, myristic acid; PFOA, perfluorooctanoic acid; POTE, polyoxyethylene (10) tridecyl ether; PTFE, polytetrafluoroethylene; SDBS, sodium dodecylbenzenesulfonate

D98-20BS-P concentration in benzyl alcohol (**Figure 3**a, Figure S6, Supporting Information) which can be primarily attributed to a higher interfacial area coverage by the Aquivion[TM] D98-20BS-P particles. However, catastrophic foam collapse occurs after 2 h at the highest concentration (5 wt%), which can be attributed to a decrease of Gibbs elasticity of the foam film in line with the phenomena observed for surfactant-stabilized foams.[24] The half-life time of the foam reaches 6 h at 1 wt% of Aquivion[TM] D98-20BS-P. The bubbles are polydisperse in size with diameters ranging from 40 to 310 µm (Figure 3b).

Evaluating the foaming properties by hand shaking is sometimes complex due to limited control and low energy input along the foaming process.[25] To achieve a high-energy input in a controlled manner, a high-speed homogenizer (IKA Ultra-TurraxT25) was used to produce foams in benzyl alcohol. After aeration at 16000 rpm for 3 min, two layers with different foam density appear for 0.5 and 1 wt% of Aquivion[TM] D98-20BS-P (**Figure 4**a). The bottom layer with small bubbles (marked as B) vanishes within few minutes (Figure 4b), while the upper layer (marked as F) contains foams that are stable for at least 4 h (Figure 4c). The initial foam volume ($V_{foam+bubble}/V_{liquid} = 1.26$) is much higher than that achieved by hand shaking ($V_{foam}/V_{liquid} = 0.63$) for 5 wt% of Aquivion[TM] D98-20BS-P, but a faster foam collapse rate is observed. This can be explained by a loosely covered interface in the latter case.

2.2.3. Extension to Other Solvents

To further confirm the role of hydrogen bond interactions between sulfonic acid groups and the solvent, we investigated
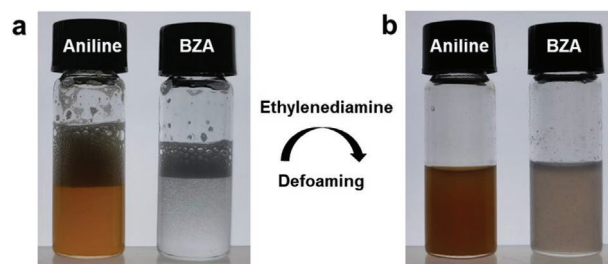

Figure 2. Foams stabilized in aniline and benzyl alcohol by 1 wt% Aquivion[TM] D98-20BS-P before and after addition of ethylenediamine.
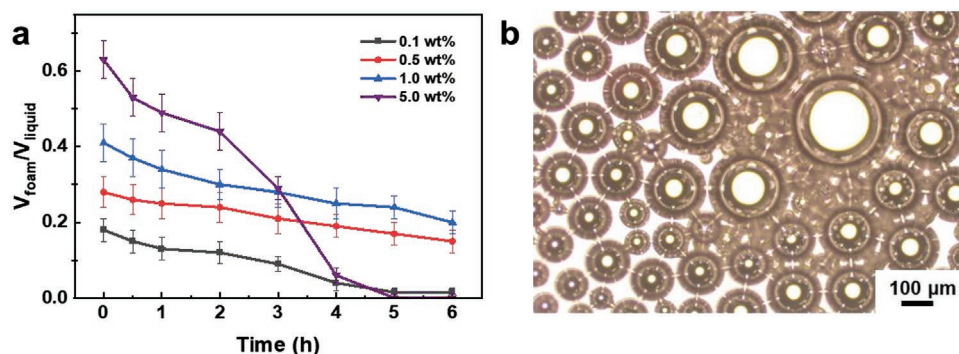
Figure 3. a) Time-evolution of the foam volume and b) optical microscopy image of bubbles in benzyl alcohol stabilized by 1 wt% Aquivion™ D98-20BS-P.

the foaming behavior of Aquivion™ D98-20BS-P in a variety of solvents ranging from non-polar hydrocarbons to polar organic solvents and water (**Figure 5**, **Table 2**). Moderately strong bases such as ethylenediamine (ED) (Table 2, entry 1) and 1-butylamine (BuA) (Table 2, entry 2) disfavor foam formation. In contrast, weakly basic aniline (pK_b = 9.3) displays an outstanding performance, with much higher foam volume and lifetime compared to benzyl alcohol (V_{foam}/V_{liquid} = 0.63; lifetime > 12 h for aniline vs V_{foam}/V_{liquid} = 0.41; lifetime = 6 h for benzyl alcohol; Table 2, entries 3–4). However, as in the case of benzyl alcohol, foams in aniline are completely destabilized after the addition of

ethylenediamine, forming a turbid suspension (Figure 2). These results suggest that intermolecular hydrogen bond interactions between $-SO_3H$ groups in Aquivion™ D98-20BS-P and the $-NH_2$ group in aniline can contribute to foam stabilization. Indeed, the $-NH_2$ group can act simultaneously as proton acceptor (N···HB) and donor (N–H···B, B stands for an acceptor) in H-bonded complexes.[26] As a matter of fact, N–H···O bonds are known to be stronger than O–H···O hydrogen bonds, which can explain the better foaming properties of aniline compared to benzyl alcohol.[27]

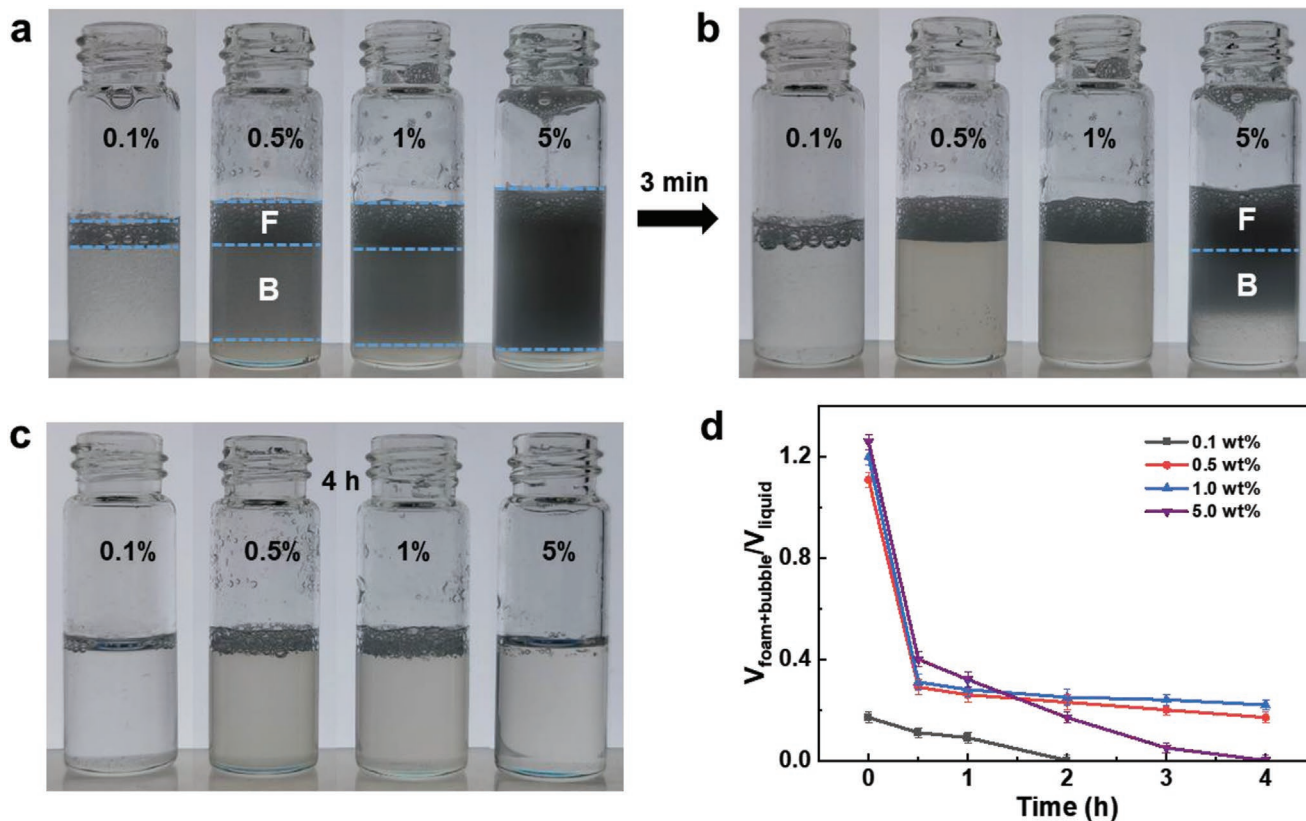In analogy to benzyl alcohol, Aquivion™ D98-20BS-P exhibits good foaming properties in acetophenone (AP)

Figure 4. a) Images of foams produced in benzyl alcohol by Ultra-Turrax at variable Aquivion™ D98-20BS-P concentration taken after preparation, b) 3 min and c) 4 h, and d) time-evolution of the foam and bubble volume. The foam volume was homogeneous within the flask in all the measurements.
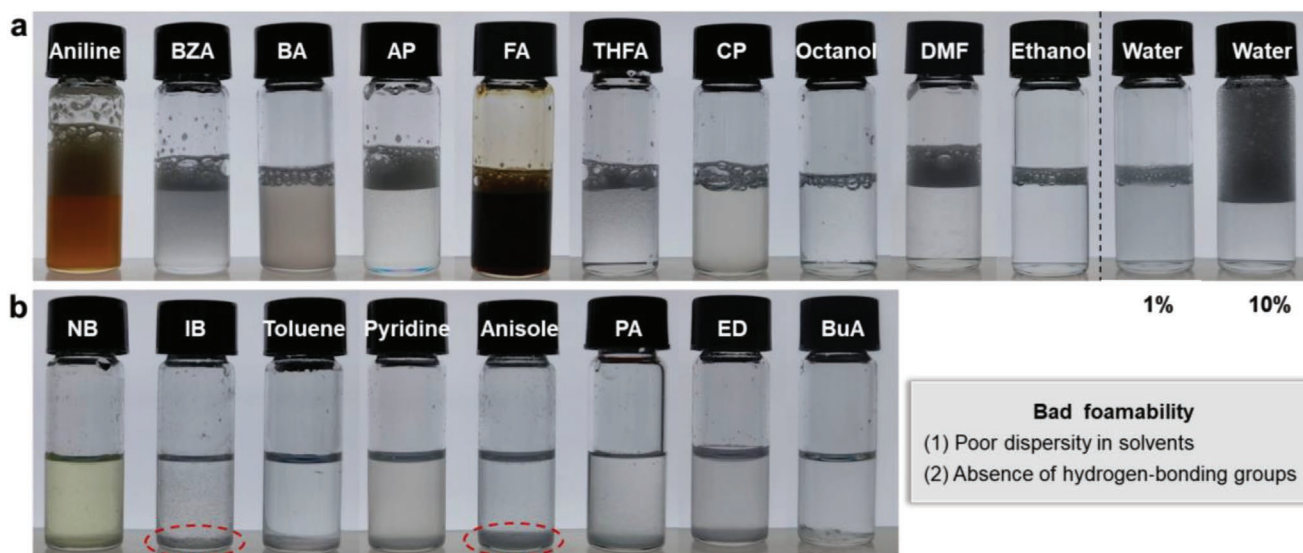
Figure 5. Images of vials with different solvents and Aquivion™ D98-20BS-P (1 wt%) after hand shaking. The foam volume was homogeneous within the flask in all the measurements.

(V_{foam}/V_{liquid} = 0.46; lifetime = 1 h; Table 2, entry 5), which has been extensively used as H-bond acceptor.[28] Lower foam volume and lifetime is obtained in cyclopentanone (CP) (Table 2, entry 6), alcohols such as tetrahydrofurfuryl alcohol (THFA) and furfuryl alcohol (FA) (Table 2, entries 7, 8), and polar solvents such as dimethyl-formamide (DMF) and water (Table 2, entries 9, 10). The foam volume obtained with 1 wt% Aquivion™ D98-20BS-P in water is relatively low, but can be drastically increased when the concentration rises to 10 wt% (Figure 5a). Other protic solvents such as 1-octanol and ethanol with low surface tension (22.3 and 27.6 mN m^{-1}, respectively) can assist hydrogen bonding,[29] but show poorer foaming properties (V_{foam}/V_{liquid} = 0.10 and 0.18, respectively; lifetime ≈1 min; entries 12, 13).

Finally, no foaming occurs in solvents with low hydrogen bonding capacity (i.e., toluene, iodobenzene, phenyl acetate, Table 2, entries 16, 18, and 19), which cannot behave as hydrogen bond donors/acceptors (Figure 5b). Moreover, poor dispersion of Aquivion™ D98-20BS-P in these solvents (red dashed line) is responsible for bad foamability.

Nitrobenzene is an interesting example to explore the role of hydrogen bond interactions, as its surface tension is similar to that of well-foaming aniline (43.9 and 43.4 mN m^{-1}, respectively). No foam is indeed obtained in nitrobenzene due to the poor hydrogen bonding capacity of nitro groups (Table 2, entry 17),[30] and bad dispersion of Aquivion™ D98-20BS-P.

Overall, the results above point out that hydrogen bond interactions exert a marked effect on foam formation. Stable foams can be generated in solvents with high hydrogen bonding capacity. Solvent molecules at the G–L interface are expected to interact with the sulfonic acid head groups of Aquivion™ D98-20BS-P by hydrogen bonding, while the oleophobic backbone prefers to stay in air (Figure S7, Supporting Information). The stronger hydrogen bonding between the solvent and Aquivion™ D98-20BS-P is favorable for foaming.
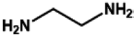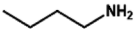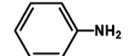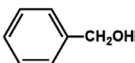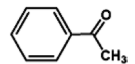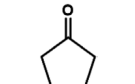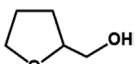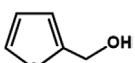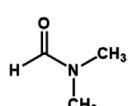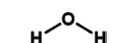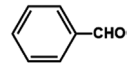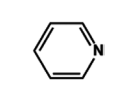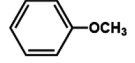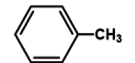
2.2.4. Effect of Temperature

The temperature is an important parameter that can affect the foaming properties of surface-active particles and the rate of chemical reactions.[31] Exploring the foaming performance of Aquivion™ D98-20BS-P at different temperatures is of great significance for conceiving applications in catalysis. Foams in benzyl alcohol and aniline are stable at 25 °C during at least 4 h (**Figure 6**, Figure S8a, Supporting Information). Rising the temperature from 25 to 80 °C results in a remarkable decline of the foamability of Aquivion™ D98-20BS-P in aniline (Figure S8b, Supporting Information). This is possibly due to formation of an insoluble aniline/acid salt,[32] which is evidenced by the formation of a precipitate on the bottom of the glass vial (Figure S8c, Supporting Information). Nonetheless, the foam lifetime is still longer than 4 h. In the case of benzyl alcohol, the foam volume increases with the temperature, whereas the half-life time decreases dramatically. Indeed, higher temperature can reduce the liquid surface tension, rendering Aquivion™ D98-20BS-P adsorption at the G–L interface less energetically favorable.[33] Besides, the decline of the benzyl alcohol viscosity with temperature,[33a] and concomitant liquid film thickness fluctuation can lower foam stability. The viscosity of the liquid film can also be reduced, which speeds up the kinetics of destabilization and shortens the half-life time.[31c]
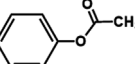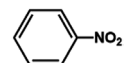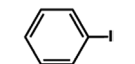
2.3. Catalytic Study in Foams Stabilized by Aquivion™ D98-20BS-P

Owing to its unique structure, Aquivion™ D98-20BS can behave concomitantly as foaming agent and acid catalyst. Taking advantage of these properties, we developed a strategy for running one-pot cascade deacetalization–hydrogenation reactions in aqueous foams. The reactions involve two sequential steps: first, benzaldehyde dimethyl acetal is hydrolyzed by Aquivion™ D98-20BS to generate benzaldehyde; second,

Table 2. Volume and half-life time of foams in solvents with different surface tensions in the presence of 1 wt% Aquivion™ D98-20BS-P.

Entry	Solvent	Structure	Surface tension [mN m^{-1}, 20 °C]	V_{foam}/V_{liquid}[a]	Foam half-life time[b]
1	Ethylenediamine (ED)		42	0	0
2	1-Butylamine (BuA)		23	0	0
3	Aniline		43.4	0.80	> 12 h
4	Benzyl alcohol (BZA)		39.5	0.41	6 h
5	Acetophenone (AP)		39.04	0.46	1 h
6	Cyclopentanone (CP)		33.1	0.29	1 h
7	Tetrahydrofurfuryl alcohol (THFA)		38.3	0.27	40 min
8	Furfuryl alcohol (FA)		38	0.25	40 min
9	Dimethylformamide (DMF)		37.1	0.49	20 min
10	Water		72.8	0.17	20 min
11	Benzaldehyde (BA)		40	0.18	≈2 min
12	1-Octanol		27.6	0.10	≈1 min
13	Ethanol		22.3	0.18	≈1 min
14	Pyridine		38	0	0
15	Anisole		35	0	0
16	Phenyl acetate (PA)		34.9	0	0
17	Nitrobenzene (NB)		43.9	0	0
18	Iodobenzene (IB)		39.7	0	0
19	Toluene		28.4	0	0

[a]V_{foam}/V_{liquid} ("foamability") = foam volume/initial volume of the solvent; [b]The foam half-life time is the time when the foam height decreased to half its original value.
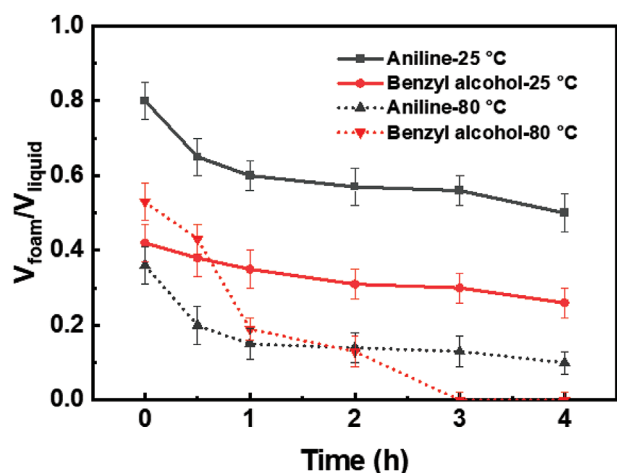
Figure 6. Time-evolution of foam volume at 25 °C and 80 °C in the presence of 1 wt% Aquivion™ D98-20BS-P after hand shaking.

homemade Pd/SiO$_2$ (4 nm Pd size, Figure S9, Supporting Information) to catalyze the hydrogenation of the intermediate product to benzyl alcohol (see details in Experimental Section). To elucidate the effect of foam (amount of G–L interface) and acidity on the catalytic activity, the hydrogenation of benzaldehyde was first carried out. Afterward, we evaluated the performance of the cascade reaction starting from benzaldehyde dimethyl acetal at optimized reaction/foaming conditions.

2.3.1. Effect of Foam and Acidity on Benzaldehyde Hydrogenation

As shown in the foaming studies above (Table 2), Aquivion™ D98-20BS-P exhibits excellent foamability in water (at 10 wt% loading). Based on these results, we carried out benzaldehyde hydrogenation in the presence of foam stabilized by Aquivion™ D98-20BS-P, and including Pd/SiO$_2$ as hydrogenation catalyst.

For comparison, we conducted a series of control experiments with/without foam using different surfactants and strong acid (TFSA) to assess the benefits of the foam system and rationalize the influence of the H$_2$–water interface on the catalytic properties (**Table 3**, Figure S10, Supporting Information).

We first carried out the reaction without foam in the presence of solely Pd/SiO$_2$ (0.5 wt%) as catalyst. The yield of benzyl alcohol reaches of 35% within 20 min (Table 3, entry 1). Adding POTE or SDBS (10 wt%) favors the generation of foam, but the yield of benzyl alcohol exhibits low increase compared to no foam system (Table 3, entries 2–3). Meanwhile, lower yield (18%) is achieved using a mixture of cationic surfactant DTAB and Pd/SiO$_2$ at the same reaction conditions (Table 3, entry 4). We then measured the catalytic performance using Aquivion™ D98-20BS-P (10 wt%) and Pd/SiO$_2$ (0.5 wt%) as catalysts in foam, affording 85% yield at the same reaction conditions (Table 3, entry 5). This body of results suggests that the simultaneous presence of foam and acid can enhance the catalytic activity for benzaldehyde hydrogenation.

To rationalize the variable catalytic efficiency of the different systems, we measured the zeta potential of Pd/SiO$_2$ particles in suspension (Table S1, Supporting Information). The cationic surfactant is expected to absorb on the silica surface due to the positive charge of the –NH$_4^+$ group in DTAB molecules.[34] After adding DTAB, the zeta potential is reversed and the surface charge of Pd/SiO$_2$ particles becomes positive (+34.3 mv vs −42.4 mv), suggesting formation of a surfactant double layer on their surface (Table S1, entries 1 and 6, Supporting Information). Based on this result, we hypothesize that the low catalytic activity arises from DTAB molecules restricting access of reactant molecules to the surface of Pd/SiO$_2$. However, this result does not explain the poor performance of the systems formulated with anionic and nonionic surfactants, suggesting that an additional effect (interface acidification) is responsible for the superior performance of the Aquivion™ D98-20BS-P-Pd/SiO$_2$ catalytic system (see below).

Table 3. Yield of benzyl alcohol in the hydrogenation of benzaldehyde with/without foam.

Entry	Catalyst	Yield [%]	Foam
1[a]	Pd/SiO$_2$ (blank)	35	No
2[a,b]	POTE + Pd/SiO$_2$	42	Yes
3[a,b]	SDBS + Pd/SiO$_2$	43	Yes
4[a,b]	DTAB + Pd/SiO$_2$	18	Yes
5[a,c]	Aquivion™ D98-20BS-P + Pd/SiO$_2$	85	Yes
6[a,c]	TFSA + Pd/SiO$_2$	41	No
7[a,c]	Aquivion™ PW98 + Pd/SiO$_2$	27	No
8[a,d]	TFSA + POTE + Pd/SiO$_2$	71	Yes
9[a,c]	PFOA + Pd/SiO$_2$	89	Yes

Reaction conditions. [a]benzaldehyde (0.5 mmol), Pd/SiO$_2$ (10 mg), H$_2$O (2 mL), H$_2$ (1.5 bar), 20 min, 25 °C; [b]Surfactant (POTE, SDBS or DTAB) (210 mg); [c]acid (210 μmol H$^+$); [d]TFSA (210 μmol H$^+$), POTE (210 mg). Nomenclature: DTAB, dodecyltrimethylammonium bromide; PFOA, perfluorooctanoic acid; POTE, polyoxyethylene (10) tridecyl ether; SDBS, sodium dodecylbenzenesulfonate.

It is known that hydrogenation reactions over Pd can be affected by the acidity of the reaction system by altering the electronic properties of Pd and activating the carbonyl group in benzaldehyde (i.e., by shifting the electron density to the O atom in C=O).[35] Adding a strong homogeneous acid, i.e., trifluoromethanesulfonic acid (TFSA), at the same number of H+ equivalents as Aquivion™ D98-20BS-P in entry 5 (210 μmol H+), to a dispersion of Pd/SiO$_2$ (0.5 wt%) results in only slight increase of the benzyl alcohol yield from 35% (Table 3, entry 1) without TFSA to 41% (Table 3, entry 6) after 20 min reaction. Likewise, adding Aquivion™ PW98 with bad dispersion in water and no foaming, affords a yield of only 27% (Table 3, entry 7). However, adding TFSA to a mixture of Pd/SiO$_2$ and non-ionic surfactant POTE enhances the yield of benzyl alcohol from 42% (Table 3, entry 2) to 71% (Table 3, entry 8). We further carried out the reaction with a perfluorinated acid (PFOA) (210 μmol H+), and Pd/SiO$_2$ (0.5 wt%), which affords good foaming properties and a yield of benzyl alcohol of 89% (Table 3, entry 9).

Overall, this body of results points out that the simultaneous presence of foaming and strong acid enhances the catalytic activity of Pd/SiO$_2$ for benzaldehyde hydrogenation, which is driven most likely by acidification of the H$_2$–water interface and its interaction with Pd/SiO$_2$.

2.3.2. Effect of Reaction Time and Aquivion™ D98-20BS-P Concentration on Cascade Reaction

Encouraged by the catalytic results above, we investigated different foam systems for the one-pot cascade deacetalization–hydrogenation reaction using benzaldehyde dimethyl acetal as reactant. As shown in **Figure 7**b, the combination of Aquivion™ D98-20BS-P and Pd/SiO$_2$ catalysts is effective for the synthesis of benzyl alcohol (84% yield) via a one-pot cascade protocol. Interestingly, a similar yield of benzyl alcohol (85%) is achieved from the hydrogenation of benzaldehyde (Table 3, entry 5), reflecting that the second step (hydrogenation) is rate determining of the overall cascade reaction.

When TFSA and Pd/SiO$_2$ are used as catalysts in non-foam conditions, the yield of benzyl alcohol is only 40% within 20 min. Adding the surfactant POTE to the above catalytic system enables the generation of aqueous foams (Figure 7a), thereby boosting the yield of benzyl alcohol to 69%. Likewise, by combining PFOA with Pd/SiO$_2$ as catalysts, a high yield of benzyl alcohol (87%) is obtained in detriment of the undesired by-product (10% yield of toluene). In contrast, only a trace amount of toluene is present in the catalytic system consisting of Aquivion™ D98-20BS-P and Pd/SiO$_2$ catalysts.

Figure S11 (Supporting Information) plots the time-evolution of the products under foaming conditions in the presence of Aquivion™ D98-20BS-P and Pd/SiO$_2$ catalyst. The initial yield of benzyl alcohol increases monotonously with the reaction time until a maximum value of 84% after 20 min, and decreases further after this time in detriment of the toluene yield.

By increasing the Aquivion™ D98-20BS-P concentration from 5 to 10 wt%, the foam volume increases by ≈50% (Figure S12b, Supporting Information). Meanwhile, the yield of benzyl alcohol increases from 47% to 84% (Figure S12a,
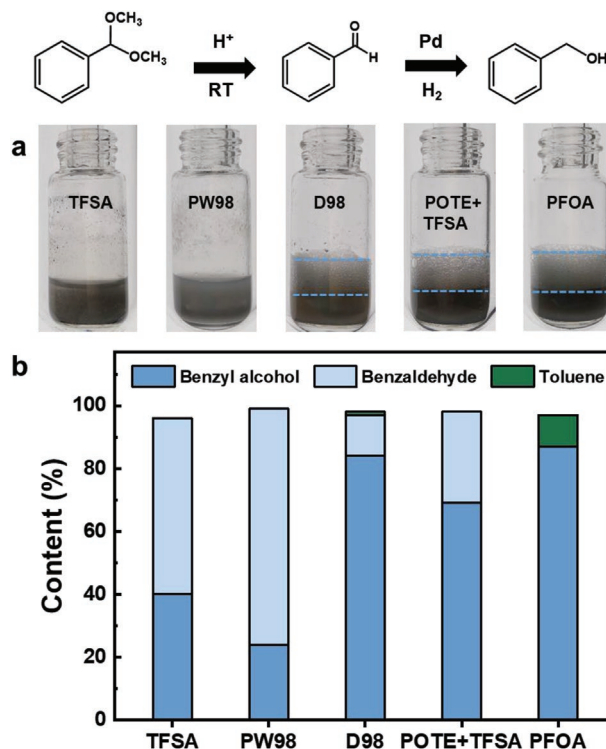

Figure 7. a) Appearance of reaction systems containing different catalysts and b) composition in different systems for the cascade reaction. Same reaction condition as those used in benzaldehyde hydrogenation, except that benzaldehyde dimethyl acetal was used as substrate.

Supporting Information). Further increase of the Aquivion™ D98-20BS-P concentration to 15% results in almost no change of yield, which is consistent with foam generation. Overall, these results point out that the catalytic performance is directly related to the volume of foam produced in the reaction system.

3. Conclusion

In this study, we unveiled the surface-active properties of Aquivion™ D98-20BS-P for stabilizing foams in a variety of organic solvents and water. Aquivion™ D98-20BS-P is able to interact with solvent molecules (e.g., benzyl alcohol, aniline, water) through hydrogen bonding, facilitating the generation of stable foams. In particular, Aquivion™ D98-20BS-P outperformed polytetrafluoroethylene, fluorinated particles and other common stabilizers, both in terms of foamability and foam stability.

Taking advantage of the excellent foaming properties and acid nature of Aquivion™ D98-20BS-P, we developed a foam system for one-pot cascade deacetalization–hydrogenation reactions. The combination of Aquivion™ D98-20BS-P and Pd/SiO$_2$ catalysts achieved remarkable performance compared to a multiphase system without foam. The enhanced reaction efficiency was attributed to a marked increase in interfacial area of the foaming system and the preferential location of catalytic acid centers at the gas–liquid interface.

Overall, this study broadens the scope of fluorinated materials as foam stabilizers and interfacial catalysts for multiphase reactions. The fundamental insights from this study pave the way for engineering novel gas-liquid-solid microreactors.

4. Experimental Section

Materials: Ethanol (95%), ethyl acetate (98%), ammonium hydroxide ($NH_3 \cdot H_2O$, 25–28%), sodium borohydride ($NaBH_4$, 98%), dodecyltrimethylammonium bromide (DTAB, 99%), sodium dodecyl sulfate (99%, SDS), acetophenone (AP, 99%), anisole (99%), phenyl acetate (PA, 99%), ethylbenzene (EB, 98%), toluene (99.5%), tetrahydrofurfuryl alcohol (THFA, 98%), cyclopentanone (CP, 97%), 1-octanol (99%), ethylenediamine (ED, 99%), 1-butylamine (BuA, 99%), and sodium hydroxide (NaOH, 96%) were purchased from Sinopharm Chemical Reagent Co., Ltd. Sodium dodecylbenzenesulfonate (SDBS), polyoxyethylene (10) tridecyl ether (POTE), and myristic acid (MA, 99%) were purchased from Sigma-Aldrich. Polytetrafluoroethylene (PTFE, 5 μm particle size) was procured from Aladdin. Acetone-d6 (99.9 atom%D) was obtained from Adamas-beta. Sodium tetrachloropalladate(II) (Na_2PdCl_4, 99.9%), benzaldehyde dimethyl acetal (97.5%), benzyl alcohol (BZA, 99.5%), benzaldehyde (BA, 98%), nitrobenzene (NB, 99%), aniline (99%), iodobenzene (IB, 97.5%), pyridine (99%), furfuryl alcohol (FA, 98%), *N,N*-dimethylformamide (DMF, 99.8%), perfluorooctanoic acid (PFOA, 98%), and trifluoromethanesulfonic acid (TFSA, 99%) and (3-aminopropyl) triethoxysilane (APTES, 98%) were purchased from J&K.

Aquivion™ D98-20BS dispersion in water (solid content: 19.3 wt%; density: 1.15 g mL^{-1} at 20 °C; acid loading: 1.0 mmol g^{-1}; equivalent weight: 980–1020 g equiv.$^{-1}$) and Aquivion™ PW98 in powder form (equivalent weight: 980–1020 g equiv.$^{-1}$, acid loading: 1.0 mmol g^{-1}), were kindly provided by Solvay.

Preparation of Pd/SiO$_2$ Catalyst: The Pd/SiO$_2$ catalyst was synthesized in three steps: (1) preparation of silica particles by the Stöber method, (2) surface modification of silica particles with amino groups, and (3) immobilization of palladium nanoparticles on the silica particles.

Monodisperse silica particles were prepared by a modified Stöber method.[36] Briefly, 3 mL of TEOS were added to a mixture of 37 mL of ethanol, 5 mL of water and 1.6 mL of ammonia hydroxide solution (28%) in a glass flask. After mixing at 40 °C for 2 h, the silica particles were collected by centrifugation and washed three times with ethanol and water.

To functionalize the surface of silica particles with amino groups, 0.6 g of silica particles was dispersed in 50 mL of ethanol by sonication in a water bath. Then, 0.3 mL of APTES was added under stirring. After stirring continuously for 24 h at room temperature, the product was separated by centrifugation and washed with ethanol. After drying at 80 °C overnight, amino-functionalized silica particles were obtained.

Palladium was further supported over the amino-functionalized silica by conventional impregnation and subsequent NaBH$_4$ reduction.[37] First, 0.5 g of aminated SiO$_2$ particles were dispersed in a mixture of 20 mL of ethanol and 15 mL of H$_2$O by ultrasonication. Then a solution of Na$_2$PdCl$_4$ (1 mL, 14 mg mL^{-1}) was added into this suspension and stirred at room temperature for 30 min. Afterward, an aqueous NaBH$_4$ solution (4 mL, 100 × 10^{-3} M) was slowly added into the mixed solution. After 2 h stirring, the solid was separated by centrifugation and washed with a mixture of water and ethanol (1:5). Finally, the resulting Pd/SiO$_2$ catalyst (0.9 wt% Pd as measured by ICP analysis) was obtained after drying at 80 °C overnight.

Preparation of Foams: The foams were first prepared by hand shaking (low energy method). Typically, 2 mL of solvent and 20 mg of solid stabilizer (1 wt%) were added into a 4-mL glass vial. After ultrasonication for 10 min, the vial was sealed and vigorously hand shaken for 30 s to generate foams.

Foams were also prepared using a high-speed homogenizer (IKA Ultra-Turrax T25 equipped with a S25N-8G dispersing tool). In these tests, a given amount of solid samples was dispersed in 2 mL of benzyl alcohol, and the dispersion was aerated at 16, 000 rpm for 3 min.

The resulting foams were kept static in front of a light board to obtain good contrast and measure the foamability or initial foam volume/liquid volume (time = 0), and then monitor the time-evolution of the foam volume to assess its stability. The foams generated with Aquivion™ D98-20BS (1 wt%) were placed on the glass microscope slides, and the images were captured with an Olympus IX-51 light transmission microscope equipped with 10 × ocular, 4 × and 10 × objectives. Olympus cellSens Standard software was used to collect bubble images, while ImageJ software was applied to quantify the size of bubbles.

General Procedure for One-Pot Cascade Reaction: The cascade reaction of benzaldehyde dimethyl acetal to benzyl alcohol was carried out as follows: 10 mg of Pd/SiO$_2$ catalyst, 0.5 mmol of benzaldehyde dimethyl acetal, 2 mL of H$_2$O and 210 mg of Aquivion™ D98-20BS-P (≈10 wt%) were added into a 10 mL glass vial. The glass vial was placed in a batch reactor (150 mL). After purging several times with H$_2$, the pressure was raised to 1.5 bar, and the reaction was carried out at room temperature under a stirring rate of 700 rpm. After the reaction, an aqueous NaOH solution (1.25 M) was added until neutral pH, the mixture was then extracted with ethyl acetate and analyzed by gas chromatography using an Agilent 7890 GC equipped with a HP-5 capillary column (30 m × 0.32 mm, 0.25 μm film thickness). Besides, the catalytic activity for the second hydrogenation step alone was investigated at the same reaction conditions using benzaldehyde as reactant.

Characterization Methods: The morphology of silica particles was investigated by transmission electron microscopy (TEM) using a JEOL JEM-2100 microscope operating at 200 kV.

Thermogravimetric analysis (TGA) was carried out on a TA SDT Q600 Instrument by heating the samples from the room temperature to 900 °C at a rate of 10 °C min^{-1} in air.

Fourier-transform infrared (FT-IR) spectra were recorded using a Thermo Scientific Nicolet iS50 equipped with an ATR accessory and operating in the range of 400–4000 cm^{-1}. All spectra were collected with 32 scans at 4 cm^{-1} resolution.

Liquid-state ^{13}C and ^{29}Si NMR spectra were recorded on a Bruker 600 MHz instrument using acetone d$_6$ as a solvent.

X-ray photoelectron spectroscopy (XPS) was performed on a Thermo Scientific K-Alpha+ XPS instrument equipped using a micro-focused monochromatic Al Kα X-ray source (1486.6 eV).

The surface charge properties of the particles in suspension were determined in terms of the zeta potential using Malvern Zetasizer Nano ZS apparatus.

The number and weight average molecular weight (M_n and M_w) of Aquivion™ D98-20BS dispersions was measured by gel permeation chromatography on a Malvern GPCmax instrument equipped with Waters Styragel HT column eluted with *N,N*-dimethylacetamide (DMAc) containing 0.01 M LiBr at a flow rate of 0.8 mL min^{-1}, which was calibrated with standard polystyrene samples.

The surface tension of the particles was measured using a force tensiometer with a Pt Wilhelmy plate (Sigma 700, Biolin Scientific) at 25 °C. The plate was flushed with ethanol before burning with a heat gun to ensure proper cleaning. The surface tension was measured three times to ensure reproducibility.

The Pd content of Pd/SiO$_2$ catalyst was quantified using inductively coupled plasma-optical emission spectroscopy (ICP-OES 5800, Agilent Technologies). Before the measurements, the samples were dissolved using a HNO$_3$/HF solution.

Statistical Analysis: All the experiments were replicated at least three times, and the data points were represented as mean ± standard deviation. The statistical analysis was carried out using one-way ANOVA to determine differences between groups, and differences between the conditions were considered significant at $p < 0.05$.

Supporting Information

Supporting Information is available from the Wiley Online Library or from the author.

[1] a) S. K. Bhargava, J. Tardio, J. Prasad, K. Föger, D. B. Akolekar, S. C. Grocott, *Ind. Eng. Chem. Res.* **2006**, *45*, 1221; b) H. P. Gemoets, Y. Su, M. Shang, V. Hessel, R. Luque, T. Noel, *Chem. Soc. Rev.* **2016**, *45*, 83; c) L. Wang, D. Fang, Y. Wang, H. Tian, J. Liu, W. Ren, *Chem. Eng. J.* **2018**, *346*, 369.

[2] a) Y. T. Shah, *Gas-Liquid-Solid Reactor Design*, McGraw-Hill, NY, USA **1979**; b) P. A. Ramachandran, R. V. Chaudari, *Three-Phase Catalytic Reactors, Topics in Chemical Engineering*, Vol *2*, Chapter 9, Gordon and Breach Science Publishers, Philadelphia, USA **1983**; c) P. Trambouze, J. P. Euzen, *Chemical Reactors: From Design to Operation*, Editions Technip, Paris, France **2004**; d) K-D. Henkel, *Reactor Types and their Industrial Applications, Ullmann's Encyclopedia of Industrial Chemistry*, Vol. *31*, Wiley-VCH, Weinheim, Germany **2012**, pp. 293-327.

[3] a) J. C. Charpentier, *Adv. Chem. Eng.* **1981**, *11*, 2; b) Y. T. Shah, B. G. Kelkar, S. P. Godbole, W-D. Deckwer, *AIChE J.* **1982**, *28*, 353; c) E. Harnby, M. F. Edwards, E. W. Nienow, *Mixing in the process industries*, Butterworth-Heinemann, London **1985**; d) A. A. C. M. Beenackers, W. P. M. Van Swaaij, *Chem. Eng. Sci.* **1993**, *48*, 3109; e) D. W. Green, R. H. Perry, in *Perry's Chemical Engineers' Handbook*, 8th ed., McGraw-Hill Professional Publishing, New York **2008**, Ch. 19; f) V. G. Pangarkar, In: *Design of Multiphase Reactors*, Chapter 8, *317*, Wiley, Weinheim **2014**.

[4] a) J. Kobayashi, Y. Mori, K. Okamoto, R. Akiyama, M. Ueno, T. Kitamori, S. Kobayashi, *Science* **2004**, *304*, 1305; b) M. Irfan, T. N. Glasnov, C. O. Kappe, *ChemSusChem.* **2011**, *4*, 300; c) B. Gutmann, D. Cantillo, C. O. Kappe, *Angew. Chem., Int. Ed.* **2015**, *54*, 6688; d) M. Reif, R. Dittmeyer, *Catal. Today* **2003**, *82*, 3; e) N. Mase, T. Mizumori, Y. Tatemoto, *Chem. Commun.* **2011**, *47*, 2086.

[5] a) H. Zhao, H. Sun, N. Qi, Y. Li, *Colloids Surf., A* **2018**, *551*, 165; b) A.-L. Fameau, A. Saint-Jalmes, *Adv. Colloid Interface Sci.* **2017**, *247*, 454; c) J. A. Rodrigues, E. Rio, J. Bobroff, D. Langevin, W. Drenckhan, *Colloids Surf., A* **2011**, *384*, 408; d) B. P. Binks, B. Vishal, *Adv. Colloid Interface Sci.* **2021**, *291*, 102404.

[6] a) B. P. Binks, T. S. Horozov, *Angew. Chem., Int. Ed.* **2005**, *44*, 3722; b) L. Braun, M. Kühnhammer, R. von Klitzing, *Curr. Opin. Colloid Interface Sci.* **2020**, *50*, 101379; c) E. Weißenborn, B. Braunschweig,

Soft Matter **2019**, *15*, 2876; d) B. P. Binks, H. Shi, *Langmuir* **2020**, *36*, 991; e) R. G. Alargova, D. S. Warhadpande, V. N. Paunov, O. D. Velev, *Langmuir* **2004**, *20*, 10371.

[7] C. Blázquez, E. Emond, S. Schneider, C. Dalmazzone, V. Bergeron, *Oil Gas Sci. Technol.* **2014**, *69*, 467.

[8] B. P. Binks, A. Rocher, *Phys. Chem. Chem. Phys.* **2010**, *12*, 9169.

[9] a) B. P. Binks, A. T. Tyowua, *Soft Matter* **2013**, *9*, 834; b) B. P. Binks, A. Rocher, M. Kirkland, *Soft Matter* **2011**, *7*, 1800; c) B. P. Binks, S. K. Johnston, T. Sekine, A. T. Tyowua, *ACS Appl. Mater. Interfaces* **2015**, *7*, 14328; d) B. P. Binks, T. Sekine, A. T. Tyowua, *Soft Matter* **2014**, *10*, 578.

[10] a) A.-L. Fameau, Y. Ma, M. Siebenbuerger, B. Bharti, *J. Colloid Interface Sci.* **2021**, *600*, 882; b) X. Bai, N. Song, L. Wen, X. Huang, J. Zhang, Y. Zhang, Y. Zhao, *Green Chem..* **2020**, *22*, 895; c) A. Feng, D. Dedovets, Y. Gu, S. Zhang, J. Sha, X. Han, M. Pera-Titus, *J. Colloid Interface Sci.* **2022**, *617*, 171.

[11] Z. Huang, F. Li, B. Chen, G. Yuan, *Green Chem.* **2015**, *17*, 2325.

[12] J. Huang, F. Cheng, B. P. Binks, H. Yang, *J. Am. Chem. Soc.* **2015**, *137*, 15015.

[13] S. Zhang, D. Dedovets, A. Feng, K. Wang, M. Pera-Titus, *J. Am. Chem. Soc.* **2022**, *144*, 1729.

[14] a) S. Andreoli, C. Oldani, V. Fiorini, S. Stagni, G. Fornasari, S. Albonetti, *Appl. Catal., A* **2020**, *597*, 117544; b) F. Liguori, C. Oldani, L. Capozzoli, N. Calisi, P. Barbaro, *Appl. Catal., A* **2021**, *610*, 117957.

[15] a) A. Karam, K. De Oliveira Vigier, S. Marinkovic, B. Estrine, C. Oldani, F. Jérôme, *ACS Catal.* **2017**, *7*, 2990; b) A. Karam, K. De Oliveira Vigier, S. Marinkovic, B. Estrine, C. Oldani, F. Jérôme, *ChemSusChem* **2017**, *10*, 3604; c) C. Moreno-Marrodan, F. Liguori, P. Barbaro, S. Caporali, L. Merlo, C. Oldani, *ChemCatChem* **2017**, *9*, 4256.

[16] a) Y. Dou, M. Zhang, S. Zhou, C. Oldani, W. Fang, Q. Cao, *Eur. J. Inorg. Chem.* **2018**, *33*, 3706; b) Y. Dou, S. Zhou, C. Oldani, W. Fang, Q. Cao, *Fuel* **2018**, *214*, 45.

[17] a) H. Shi, Z. Fan, B. Hong, M. Pera-Titus, *ChemSusChem* **2017**, *10*, 3363; b) W. Fang, Z. Fan, H. Shi, S. Wang, W. Shen, H. Xu, J.-M. Clacens, F. De Campo, A. Liebens, M. Pera-Titus, *J. Mater. Chem. A* **2016**, *4*, 4380; c) S. Zhang, B. Hong, Z. Fan, J. Lu, Y. Xu, M. Pera-Titus, *ACS Appl. Mater. Interfaces* **2018**, *10*, 26795.

[18] Q. Deng, C. Wilkie, R. Moore, K. A. Mauritz, *Polymer* **1998**, *39*, 5961.

[19] Z. Liang, W. Chen, J. Liu, S. Wang, Z. Zhou, W. Li, G. Sun, Q. Xin, *J. Membr. Sci.* **2004**, *233*, 39.

[20] a) M. Martínez de Yuso, L. Neves, I. Coelhoso, J. Crespo, J. Benavente, E. Rodríguez-Castellón, *Fuel Cells* **2012**, *12*, 606; b) W. Fang, S. Wang, A. Liebens, F. De Campo, H. Xu, W. Shen, M. Pera-Titus, J.-M. Clacens, *Catal. Sci. Technol.* **2015**, *5*, 3980.

[21] C. Chen, G. Levitin, D. W. Hess, T. F. Fuller, *J. Power Sources* **2007**, *169*, 288.

[22] E. Moukheiber, G. De Moor, L. Flandin, C. Bas, *J. Membr. Sci.* **2012**, *389*, 294.

[23] a) Q. Chen, K. Schmidt-Rohr, *Macromolecules* **2004**, *37*, 5995; b) L. Ghassemzadeh, M. Marrony, R. Barrera, K. Kreuer, J. Maier, K. Müller, *J. Power Sources* **2009**, *186*, 334.

[24] M. R. Behera, S. R. Varade, P. Ghosh, P. Paul, A. S. Negi, *Ind. Eng. Chem. Res.* **2014**, *53*, 18497.

[25] L. R. Arriaga, W. Drenckhan, A. Salonen, J. A. Rodrigues, R. Iniguez-Palomares, E. Rio, D. Langevin, *Soft Matter* **2012**, *8*, 11085.

[26] a) M. Raveendra, M. Chandrasekhar, K. C. Reddy, A. Venkatesulu, K. Sivakumar, K. D. Reddy, *Fluid Phase Equilib.* **2018**, *462*, 85; b) H. Szatyłowicz, T. M. Krygowski, *J. Mol. Struct.* **2007**, *844*, 200; c) S. Mishra, J.-L. Kuo, G. N. Patwari, *Phys. Chem. Chem. Phys.* **2018**, *20*, 21557.

[27] a) H. J. Böhm, S. Brode, U. Hesse, G. Klebe, *Chem. - Eur. J.* **1996**, *2*, 1509; b) J. Emsley, *Chem. Soc. Rev.* **1980**, *9*, 91.

[28] a) C. Dalvit, C. Invernizzi, A. Vulpetti, *Chem. - Eur. J.* **2014**, *20*, 11058; b) C. Laurence, J. Graton, M. Berthelot, F. O. Besseau, J.-Y. Le Questel, M. Luçon, C. Ouvrard, A. Planchat, E. Renault, *J. Org. Chem.* **2010**, *75*, 4105.

[29] a) S. A. Rice, A. R. Dinner, in *Advances in Chemical Physics*, Vol. *147*, **2011**, p. 2; b) E. Gawlita, M. Lantz, P. Paneth, A. F. Bell, P. J. Tonge, V. E. Anderson, *J. Am. Chem. Soc.* **2000**, *122*, 11660.

[30] a) J. M. Robinson, D. Philp, K. D. Harris, B. M. Kariuki, *New J. Chem.* **2000**, *24*, 799; b) C. A. Kingsbury, *Why Are the Nitro and Sulfone Groups Poor Hydrogen Bonders? Faculty Publications-Chemistry Department*, University of Nebraska-Lincoln, Lincoln **2015**.

[31] a) K. Oetjen, C. Bilke-Krause, M. Madani, T. Willers, *Colloids Surf., A* **2014**, *460*, 280; b) Z. Zakaria, Z. Ariff, C. Sipaut, *J. Vinyl Addit. Technol.* **2009**, *15*, 120; c) D. Li, B. Ren, L. Zhang, J. Ezekiel, S. Ren, Y. Feng, *Chem. Eng. Res. Des.* **2015**, *102*, 234; d) I. W. Smith, *Chem. Soc. Rev.* **2008**, *37*, 812.

[32] a) J. Yang, Y. Ding, J. Zhang, *Mater. Chem. Phys.* **2008**, *112*, 322; b) O. Misoon, K. Seok, *Electrochim. Acta* **2012**, *59*, 196.

[33] a) K.-D. Chen, Y.-F. Lin, C.-H. Tu, *J. Chem. Eng. Data* **2012**, *57*, 1118; b) J. Águila-Hernández, A. Trejo, B. E. García-Flores, *Colloids Surf., A* **2007**, *308*, 33.

[34] a) X.-Q. Wei, W.-J. Zhang, L. Lai, P. Mei, L.-M. Wu, Y.-Q. Wang, *J. Mol. Liq.* **2019**, *291*, 111341; b) K. Lebdioua, A. Aimable, M. Cerbelaud, A. Videcoq, C. Peyratout, *J. Colloid Interface Sci.* **2018**, *520*, 127.

[35] a) N. Lee, Y.-M. Chung, *Appl. Surf. Sci.* **2016**, *370*, 160; b) J. Huang, Y. Jiang, N. Van Vegten, M. Hunger, A. Baiker, *J. Catal.* **2011**, *281*, 352; c) Y. Song, U. Sanya, D. Pangotra, J. D. Holladay, D. M. Camaioni, O. Y. Gutierrez, J. A. Lercher, *J. Catal.* **2018**, *359*, 68.

[36] W. Stöber, A. Fink, E. Bohn, *J. Colloid Interface Sci.* **1968**, *26*, 62.

[37] a) A. Bulut, M. Yurderi, Y. Karatas, M. Zahmakiran, H. Kivrak, M. Gulcan, M. Kaya, *Appl. Catal., B* **2015**, *164*, 324; b) M. Yuan, R. Yang, S. Wei, X. Hu, D. Xu, J. Yang, Z. Dong, *J. Colloid Interface Sci.* **2019**, *538*, 720; c) M. Celebi, M. Yurderi, A. Bulut, M. Kaya, M. Zahmakiran, *Appl. Catal., B* **2016**, *180*, 53.

2200380 (11 of 11)